The Plant Cell, Vol. 27: 2530–2544, September 2015, www.plantcell.org

Colletotrichum orbiculare Regulates Cell Cycle G1/S Progression via a Two-Component GAP and a GTPase to Establish Plant Infection[OPEN]

Fumi Fukada and Yasuyuki Kubo[1]

Laboratory of Plant Pathology, Life and Environmental Sciences, Graduate School of Kyoto Prefectural University, Kyoto 606-8522, Japan

ORCID IDs: 0000-0002-6815-9929 (F.F.); 0000-0002-8600-9705 (Y.K.)

Morphogenesis in filamentous fungi depends on appropriate cell cycle progression. Here, we report that cells of the cucumber anthracnose fungus *Colletotrichum orbiculare* regulate G1/S progression via a two-component GAP, consisting of Budding-uninhibited-by-benomyl-2 (Bub2) and Byr-four-alike-1 (Bfa1) as well as its GTPase Termination-of-M-phase-1 (Tem1) to establish successful infection. In a random insertional mutagenesis screen of infection-related morphogenesis, we isolated a homolog of *Saccharomyces cerevisiae*, *BUB2*, which encodes a two-component Rab GAP protein that forms a GAP complex with Bfa1p and negatively regulates mitotic exit. Interestingly, disruption of either Co *BUB2* or Co *BFA1* resulted in earlier onset of nuclear division and decreased the time of phase progression from G1 to S during appressorium development. *S. cerevisiae* GTPase Tem1p is the downstream target of the Bub2p/Bfa1p GAP complex. Introducing the dominant-negative form of Co Tem1 into Co *bub2Δ* or Co *bfa1Δ* complemented the defect in G1/S progression, indicating that Co Bub2/Co Bfa1 regulates G1/S progression via Co Tem1. Based on a pathogenicity assay, we found that Co *bub2Δ* and Co *bfa1Δ* reduced pathogenesis by attenuating infection-related morphogenesis and enhancing the plant defense response. Thus, during appressorium development, *C. orbiculare* Bub2/Bfa1 regulates G1/S progression via Co Tem1, and this regulation is essential to establish plant infection.

INTRODUCTION

Colletotrichum orbiculare is the causal agent of cucumber anthracnose disease. The infection process is initiated upon recognition of appropriate surface cues by aseptate conidia. After the conidia germinate, the resultant germ tubes differentiate into dome-shaped appressoria and undergo nuclear division. Successful appressorium function and, thus, infection depend on the proper sequence of metabolic events, including melanin synthesis, peroxisome metabolism, establishment of cellular polarity and cell wall integrity, and signal transduction, occurring in the fungus (Kubo and Takano, 2013; Harata and Kubo, 2014). Importantly, a microtubule dynamics analysis revealed that a precise nuclear distribution inside cells is also required for normal appressorial development (Takano et al., 2001). In the rice blast fungus *Magnaporthe oryzae*, appropriate regulation of the cell cycle is necessary to establish infection. The fungus must enter the S phase to initiate appressorium formation, whereas entry into mitosis and autophagic programmed cell death in conidia are essential for the germ tube to differentiate into a functional appressorium (Veneault-Fourrey et al., 2006; Saunders et al., 2010a). In addition to cell cycle regulation, pathogenesis in *M. oryzae* also requires that cells undergo the correct number of divisions at precise locations (Saunders et al., 2010b). Thus, the progression of the cell cycle and cytokinesis seem to regulate cellular differentiation processes. However, the details of cell cycle regulation that could affect infection-related morphogenesis and pathogenesis are poorly understood in *Colletotrichum* species.

In the budding yeast *Saccharomyces cerevisiae* and the multimorphic fungus *Candida albicans*, exit from mitosis and entry into cytokinesis are regulated by the mitotic exit network (MEN), a GTPase-regulated kinase cascade (Bardin and Amon, 2001; Milne et al., 2014). The MEN consists of the central GTPase Tem1p, which is regulated by the two-component GTPase-activating protein (GAP), consisting of Bub2p and Bfa1p. In *S. cerevisiae* cells, the Bub2p/Bfa1p complex constitutes multiple cell cycle checkpoints that prevent mitotic exit (Hu and Elledge, 2002). Such checkpoints include the spindle position checkpoint (SPOC), the surveillance mechanism for proper orientation of the mitotic spindle (Yeh et al., 1995); the spindle assembly checkpoint (SAC), for proper attachment of all kinetochores to the spindle (Musacchio and Salmon, 2007); and the DNA damage checkpoint (DDC), for the proper protection of chromosomal DNA (Harrison and Haber, 2006; Valerio-Santiago et al., 2013). The fission yeast *Schizosaccharomyces pombe* and the filamentous fungus *Aspergillus nidulans* have a signaling pathway homologous to MEN, termed the septation initiation network (SIN). The primary role of this network is to regulate septation rather than mitotic exit (Bruno et al., 2001; Krapp and Simanis, 2008). The SIN consists of the GTPase Spg1 (Septum-promoting GTP binding protein 1), an ortholog of *S. cerevisiae* Tem1p, which regulates a protein kinase pathway that triggers contraction of the actomyosin ring and positively regulates septum formation (Schmidt et al., 1997). The

[1] Address correspondence to y_kubo@kpu.ac.jp.
The author responsible for distribution of materials integral to the findings presented in this article in accordance with the policy described in the Instructions for Authors (www.plantcell.org) is: Yasuyuki Kubo (y_kubo@kpu.ac.jp).
[OPEN]Articles can be viewed online without a subscription.
www.plantcell.org/cgi/doi/10.1105/tpc.15.00179

two-component GAP consists of Cdc16 and Byr4, orthologs of *S. cerevisiae* Bub2p and Bfa1p, that negatively regulate the SIN signaling pathway by inactivating the GTPase Spg1 and thus preventing septum formation during interphase (Furge et al., 1998; Li et al., 2000). Despite many of the MEN and SIN components being highly conserved in yeast and filamentous fungi, each of the homologous genes differs in its function. In plant pathogenic fungi, the functions of the GTPase Tem1 and two-component GAP consisting of Bub2 and Bfa1 have been reported only for the basidiomycete *Ustilago maydis*, indicating that the Tem1 homolog Ras3 regulates nuclear envelope breakdown rather than mitotic exit or septum formation (Straube et al., 2005), but other components or events are currently lacking in plant pathogenic fungi. Thus, the characterization of the two-component GAP and its GTPase in *C. orbiculare* could provide insight into the roles of MEN/SIN in fungal pathogenicity.

In this study, we present evidence that appropriate G1/S progression is regulated by *BUB2* and *BFA1* through *TEM1* during appressorium development and is required for typical infection-related morphogenesis and pathogenesis of *C. orbiculare.*

RESULTS

Screening for Mutants with Defects in Pathogenesis and Infection-Related Morphogenesis and Identifying Co *BUB2* in *C. orbiculare*

To identify genes involved in pathogenesis and infection-related morphogenesis, we performed random gene-insertional mutagenesis of the wild-type strain 104-T of *C. orbiculare* using *Agrobacterium tumefaciens*-mediated transformation (AtMT). We screened 10,021 mutants for defective pathogenesis and abnormal infection-related morphogenesis on cucumber (*Cucumis sativus*) cotyledons detached from plants. We obtained a mutant, named PDM1 (Pathogenicity Deficient Mutant 1), which formed only a few penetration hyphae on the surface of cotyledons and induced either no lesions or only a few, in contrast to the wild type, which formed penetration hyphae in the host cucumber leaves and induced distinct necrotic lesions on the leaves.

DNA segments adjacent to the inserted plasmid were isolated from the PDM1 mutant using a thermal asymmetric interlaced-PCR. A BLASTp search (NCBI BLAST; http://blast.ncbi.nlm.nih.gov/Blast.cgi) revealed that the sequence adjacent to the T-DNA exhibited high similarity to the amino acid sequence of Bub2p of *S. cerevisiae* and to those of the filamentous fungi (Supplemental Figure 1). This *BUB2* homolog of *C. orbiculare* was designated Co *BUB2*. Comparison of the amplified cDNA with genomic DNA verified that Co *BUB2* encodes a protein of 472 amino acids and contains the Rab GAP domain. The amino acid sequences of Co Bub2 homologs are well conserved among yeast and filamentous fungi, especially in the Rab GAP domain, which has an E-value 4.99 e-33, suggesting that Co Bub2 has potential GAP activity in *C. orbiculare*. In *S. cerevisiae*, Bub2p constitutes three surveillance cell cycle checkpoints (SPOC, SAC, and DDC), which ensure that the replicated genomic material is protected from damage and correctly distributed between the daughter and mother cells by preventing mitotic exit (Hu and Elledge, 2002).

Co Bub2/Co Bfa1 GAP Plays a Key Role in G1/S Progression during Appressorium Development

To understand the regulatory mechanism of Co *BUB2*, we focused on partner genes that interact with Co Bub2. In *S. cerevisiae*, Bub2p forms a two-component GAP complex with Bfa1p and requires Bfa1p to stimulate GTP hydrolysis of the downstream GTPase Tem1p to regulate the exit from mitosis (Geymonat et al., 2002). We identified a putative *BFA1* homolog, Co *BFA1*, by BLAST search of the *C. orbiculare* genome (Gan et al., 2013), which putatively encodes a protein of 1020 amino acids with high identity to the sequence of *S. cerevisiae* Bfa1p, with an E-value of 2e-05 (Supplemental Figure 2).

To investigate the function of Co *BUB2* and Co *BFA1*, we generated the Co *bub2Δ* and Co *bfa1Δ* targeted disruption mutants (Supplemental Figure 3). Mutation of Co *bub2* or Co *bfa1* caused slightly delayed growth and a significant defect in conidiation (Supplemental Table 1). Furthermore, the mutation caused a defect in nuclear division during appressorium formation. The conidia of the wild type contained one nucleus and, following conidial germination, underwent one round of nuclear division during appressorium development at 4 h postincubation (hpi) (Figure 1). This resulted in the conidium and appressorium each having one nucleus. At 10 hpi, the nucleus that remained in the conidium had been broken down by autophagy, while the appressorium retained its one nucleus. Surprisingly, in Co *bub2Δ* and Co *bfa1Δ*, the nucleus in the conidium divided before the conidium germinated at 2 hpi, so that the pregermination conidium had two nuclei (Figure 1). After the development of the appressorium, in some germlings one nucleus migrated into the appressorium, resulting in one nucleus in the conidium and the other in the appressorium. The other germlings underwent a second round of mitosis, resulting in multiple nuclei in the conidium and appressorium. At 10 hpi, conidial autophagy in Co *bub2Δ* and Co *bfa1Δ* was significantly delayed compared with that in the wild type. Thus, in contrast to *S. cerevisiae BUB2* and *BFA1*, Co *BUB2* and Co *BFA1* are involved in the timing of nuclear division and in the proper distribution of nuclei during appressorium development.

To investigate nuclear division and migration during appressorium development cytologically, we introduced the α-*TUBULIN-mRFP* fusion gene and *HISTONE H1-GFP* fusion gene into *C. orbiculare* to visualize microtubules and nuclei, respectively. In the wild type, microtubules were apparent at 4 to 5 hpi, that is, following appressorium development, and microtubules aligned parallel to the conidia-appressorium axis (Figure 2; Supplemental Movie 1). One spindle pole body remained in the conidium, and the other migrated into the appressorium within 6 min. In accordance with the movement of the microtubules, the mother nucleus divided; one mother nucleus remained in the conidium, while one daughter nucleus migrated into the appressorium. By contrast, in most conidia of Co *bub2Δ* and Co *bfa1Δ*, microtubules appeared at 2 hpi in the pregermination conidium, and the partner spindle pole body migrated to the edge of the conidium (Figure 2; Supplemental Movie 2). In the same way, the mother nucleus divided, and the two nuclei moved to the edge of the cell. These results confirm that mitosis of Co *bub2Δ* and Co *bfa1Δ* started ~2 h earlier than that of the wild type.

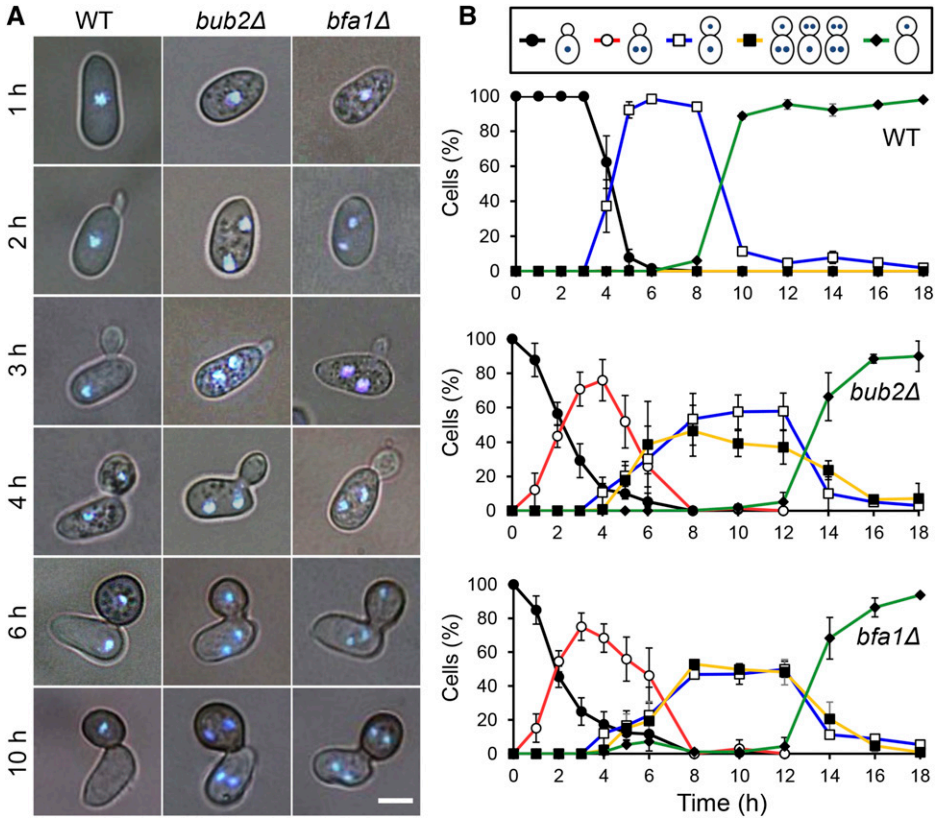

Figure 1. Co *BUB2* and Co *BFA1* Are Involved in the Timing of Initiation of Nuclear Division during Appressorium Development.

(A) Time-course series of micrographs to show nuclei in conidia and infection structures of *C. orbiculare* wild type and Co *bub2Δ* and Co *bfa1Δ* mutants during appressorium development. Staining was performed using DAPI. Bar = 5 μm.

(B) Mean percentage (±SE; $n = 3$) of cells with various patterns of nuclear distribution. Scoring: one nucleus retained in the conidium (black), two nuclei retained in the conidium (red), one nucleus in the conidium and the other in the appressorium through mitosis (blue), multiple nuclei in the conidium and appressorium through two or three rounds of mitosis (yellow), and one nucleus in the appressorium and degradation of the remaining nucleus in the conidium through autophagy (green). At least 200 conidia were scored at each time point.

We therefore hypothesized that the cell cycle of Co *bub2Δ* and Co *bfa1Δ* might progress earlier than that of the wild type. To test this hypothesis, we evaluated the time of entry into S phase, with time 0 defined as the onset of conidial incubation, in Co *bub2Δ* as a representative strain during appressorium development. We used an established method in which a chromosomal locus is tagged with a fluorescent focus by recruiting a GFP-tagged Lac repressor fusion (GFP-LacI) to an integrated Lac operator array (LacO) (Robinett et al., 1996; Straight et al., 1996) (Figure 3A). In this chromosome tagging system, the time of DNA replication (S phase) is determined based on large-scale chromatin organization; that is, cells containing prereplicated DNA exhibit a single fluorescent spot, while cells that have undergone post-DNA replication harbor closely spaced double fluorescent spots, with one on each separated sister chromatid (Straight et al., 1996). To evaluate the timing of duplication of GFP spots in *C. orbiculare* nuclei, which refers to the timing of DNA replication (S phase), we constructed the *S. pombe* LacI-NLS-eGFP fusion protein (Straight et al., 1996; Nabeshima et al., 1998). Then, an array consisting of yeast vectors harboring 256 tandem copies of LacO (Yamamoto and Hiraoka, 2003) was ectopically introduced into the strain expressing the GFP-LacI reporter fusion. In the wild-type strain containing LacO/LacI-GFP, a single GFP spot was observed at a nucleus after the onset of conidial incubation (Figures 3B and 3C). After germination at 105 min, cells containing two GFP spots started to appear and such cells represented up to ~80% of all cells by 165 min. At 240 min, mitosis was completed and each nucleus in the conidium and appressorium contained a single spot. On the other hand, in the Co *bub2Δ* mutant, a single GFP spot observed at the onset of conidial incubation decreased immediately after incubation, but double GFP spots in the nucleus were seen in up to ~50% of Co *bub2Δ* cells by 60 min (Figures 3B and 3C). These results indicate that S phase starts after around 120 min of incubation in the wild type, but before 60 min in Co *bub2Δ*. Therefore, Co Bub2/Co Bfa1 regulates G1/S progression in the cell cycle during germination and appressorium formation.

Next, we investigated whether regulation of G1/S progression by Co Bub2/Co Bfa1 is specific to morphogenesis from conidia. To test this idea, we monitored nuclear division of Co *bub2Δ* during hyphal growth in the presence of exogenous nutrients, which

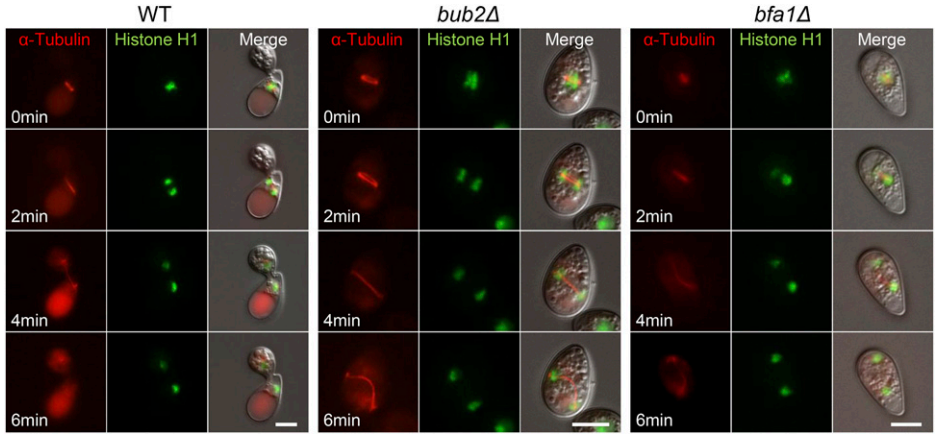

Figure 2. Earlier Mitosis of *Co bub2Δ* and *Co bfa1Δ* Visualized by Live-Cell Imaging.

C. orbiculare wild type, Co *bub2Δ*, and Co *bfa1Δ* showing microtubule dynamics and nuclear division. The *αTUBULIN-mRFP* and *HISTONE H1-GFP* gene fusion vectors were introduced into the three strains. Microtubules (red) and nuclei (green) were first observed in the appressorium-developing conidia of the wild type at 4 hpi, whereas they were first observed in the pregermination conidia in Co *bub2Δ* and Co *bfa1Δ* at 2 hpi. Bars = 5 μm.

leads to the development of vegetative hyphae without appressorium formation (Takano et al., 1997). Under these conditions, before germination at 2 hpi, one round of nuclear division occurred in Co *bub2Δ*, but not in the wild type (Supplemental Figure 4). On the other hand, from 2 to 10 hpi in the vegetative hyphae, the increase in nuclear number in Co *bub2Δ* was similar to that in the wild type. Thus, Co *BUB2* and Co *BFA1* are involved in G1/S progression in pregermination conidia, but not in vegetative

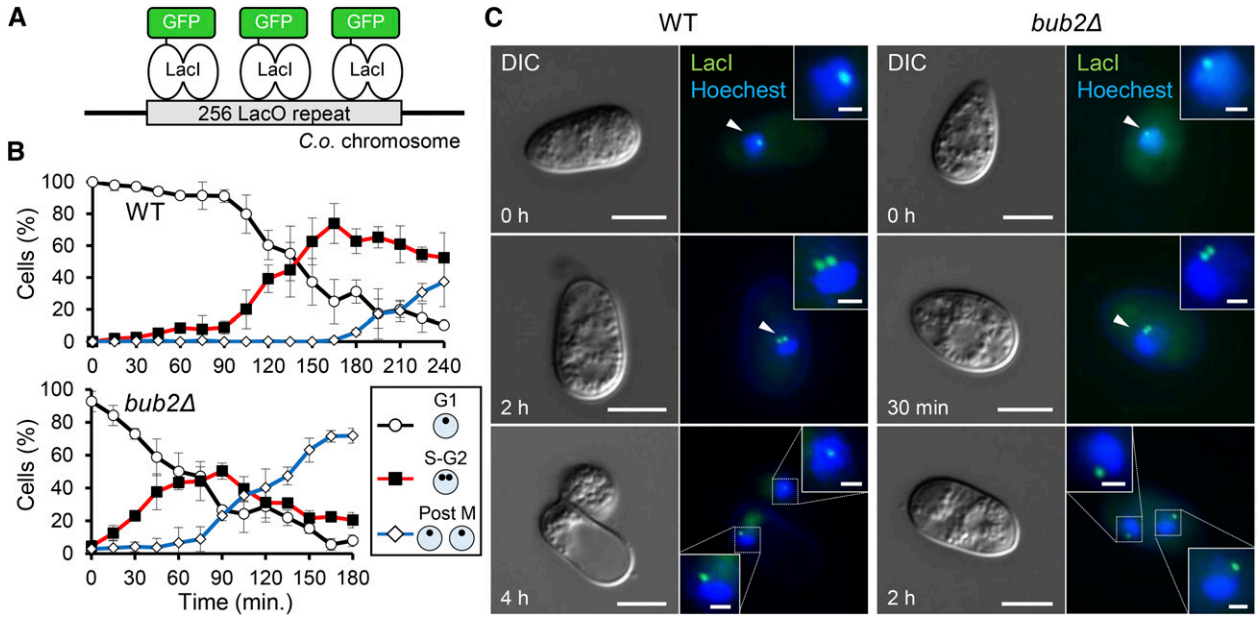

Figure 3. Co *BUB2* and Co *BFA1* Regulate G1/S Progression in *C. orbiculare*.

(A) Schematic representation of the *C. orbiculare* strain expressing GFP-LacI-NLS, which associates with the LacO array integrated into *C. orbiculare* chromosomes.

(B) Mean percentage (±SE; $n = 3$) of wild-type (WT) and Co *bub2Δ* cells with three patterns of GFP-LacI spots. Scoring: single fluorescent spot at one nucleus, putative G1 phase (black); closely spaced double spots at one nucleus, putative post-S phase or G2 phase (red); and single spots at both nuclei, putative post-M phase (blue). At least 100 conidia were scored at each time point.

(C) Representative images of LacO/LacI-GFP introduced wild type and Co *bub2Δ* during appressorium development. Enlarged images of the nucleus with one or two LacI-GFP spots are shown in the boxed areas. Arrowheads indicate interphase nuclei. Nuclear staining was performed using Hoechst 33342. Bars in DIC panels = 5 μm; bars in enlarged image = 1 μm.

hyphal growth; their involvement seems to be specific for G1/S progression during appressorium development.

Co *BUB2* and Co *BFA1* Are Orthologs of *BUB2* and *BFA1* in *S. cerevisiae*

In *S. cerevisiae*, the Bub2p/Bfa1p GAP complex negatively regulates mitotic exit, while in *C. orbiculare*, Bub2/Bfa1 regulates proper G1/S progression. We therefore examined whether Co *BUB2* and Co *BFA1* were orthologs of *BUB2* and *BFA1* of *S. cerevisiae*. We conducted a complementation test that examined whether *S. cerevisiae* Bub2p/Bfa1p GAP activity regulated G1/S progression when introduced into *C. orbiculare Co bub2Δ Co bfa1Δ* double mutants. We constructed plasmids pBIBub2B and pBIBfa1Z that express open reading frames of *S. cerevisiae BUB2* and *BFA1* under the control of the Co *BUB2* and Co *BFA1* native promoters, respectively. We transformed *Co bub2Δ Co bfa1Δ* double mutants with a combination of *S. cerevisiae BUB2* and *BFA1*. The wild-type phenotype was restored in transformants that expressed both *S. cerevisiae BUB2* and *BFA1*. While the nuclear division of *Co bub2Δ Co bfa1Δ* started earlier in pregermination conidia, the nuclear division of the transformants that expressed both *S. cerevisiae BUB2* and *BFA1* started at a similar time point to the wild type in appressorium-forming conidia (Figure 4). This result indicates that the cell cycle defect of *Co bub2Δ Co bfa1Δ* was complemented by *S. cerevisiae BUB2* and *BFA1*. Thus, we confirmed that *S. cerevisiae BUB2* and *BFA1*, which regulate mitotic exit, are orthologs of *C. orbiculare BUB2* and *BFA1*.

Co Bub2 Forms a Two-Component GAP Complex with Co Bfa1, and Co Bub2/Co Bfa1 Interacts with GTPase Co Tem1

Since our results showed that the functions of Co Bub2 and Co Bfa1 differed from those of the respective homologs in yeast, we sought to determine the downstream target of Co Bub2/Co Bfa1 that regulates G1/S progression. In *S. cerevisiae*, the Bub2p/Bfa1p GAP complex negatively regulates Ras-like GTPase Tem1p, which triggers the exit from mitosis (Geymonat et al., 2002). Tem1p is activated in the GTP-bound form, and activity of Bub2p/Bfa1p GAP decreases the amount of the active GTP-bound form of Tem1p by stimulating GTP hydrolysis. We identified a gene, Co *TEM1*, from the *C. orbiculare* genome database (Gan et al., 2013), which showed 58% sequence identity with *S. cerevisiae* Tem1p (Supplemental Figure 5). The Co Tem1 sequence displays the highly conserved Rab family domain, suggesting that Co Tem1 potentially functions as a Rab GTPase in *C. orbiculare*.

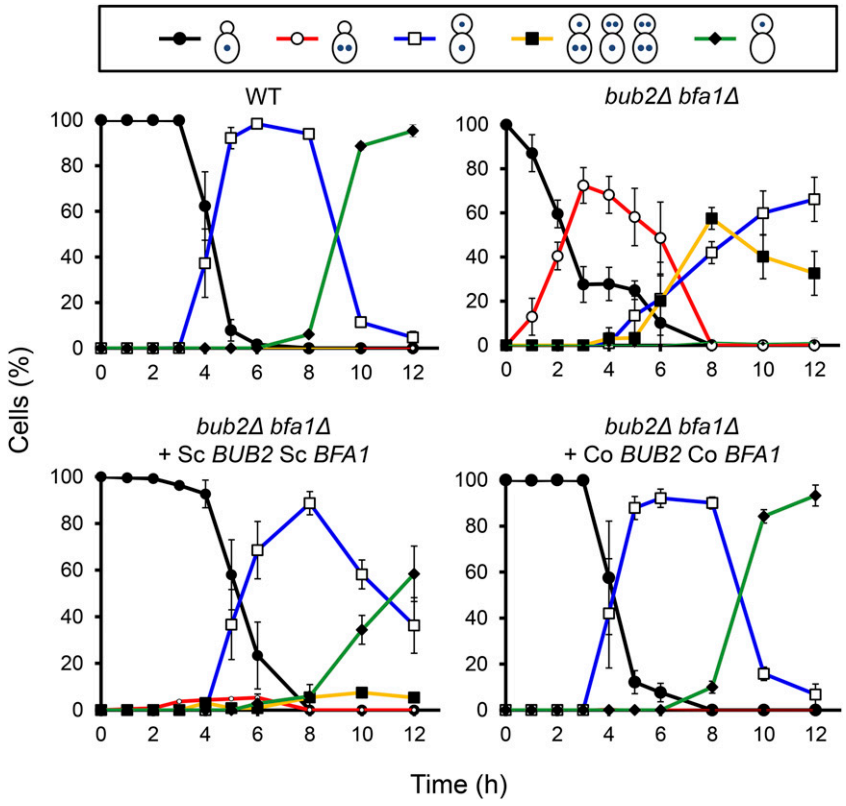

Figure 4. Co *BUB2* and Co *BFA1* Genes Are Orthologs of *BUB2* and *BFA1* of *S. cerevisiae.*

Complementation of defects in nuclear behavior in Co *bub2Δ* Co *bfa1Δ* by introducing *S. cerevisiae BUB2* and *BFA1*. Each nuclear distribution pattern was calculated (means ± SE; $n = 3$). For the positive control, the Co *bub2Δ* Co *bfa1Δ* mutant expressing Co *BUB2* and Co *BFA1* was used. At least 200 conidia were scored at each time point.

To investigate whether Co Bub2, Co Bfa1, and Co Tem1 interact with each other, we performed yeast two-hybrid assays. First, the interaction of Co Bub2 and Co Bfa1 was examined. Co Bub2 contains the highly conserved Rab GAP domain and 124 amino acids of the N-terminal region that are not conserved in *S. cerevisiae* and *S. pombe*, showing only sequence similarity to proteins of filamentous fungi (Supplemental Figures 1 and 6). In Co Bfa1, 43 amino acids of two imperfect direct repeats (IDRs) at the C-terminal end have been reported to be required for interaction with the Co Bub2 homolog in *S. pombe* (Furge et al., 1998), and the two IDRs are conserved in filamentous fungi and yeast (Supplemental Figures 2 and 6). Yeast clones carrying Co $Bfa1_{full}$ grew only in the presence of $CoBub2_{full}$ and Co $Bub2_{1-124}$ on selective medium, but not in combination with $CoBub2_{125-473}$, suggesting that Co Bfa1 interacts physically with the N-terminal region of Co Bub2 (Supplemental Figure 6). On the other hand, yeast clones carrying Co $Bub2_{full}$ grew only in the presence of Co $Bfa1_{full}$ and Co $Bfa1_{784-1020}$, but not in combination with Co $Bfa1_{1-783}$, suggesting that Co Bub2 interacts physically with the IDR region of Co Bfa1. These results suggest that Co Bub2 forms the two-component GAP complex with Co Bfa1 and that the N-terminal region of Co Bub2 and the IDR region of Co Bfa1 are required for this interaction.

Next, we investigated whether the Co Bub2/Co Bfa1 GAP complex interacts with Co Tem1 in *C. orbiculare*, similar to the yeast homologs. Co Tem1 contains the highly conserved Rab family domain, and 95 amino acids of the N-terminal region that are not conserved in *S. cerevisiae* and *S. pombe*, but it displays similarity to the filamentous fungi proteins similar to the Co Bub2 sequence (Figure 5A; Supplemental Figure 5). Yeast clones carrying Co $Bub2_{full}$ or Co $Bfa1_{full}$ grew only in the presence of Co $Tem1_{1-95}$ on selective medium, but not in combination with Co $Tem1_{96-302}$ (Figure 5B), indicating that Co Tem1 interacts physically with Co Bub2 and Co Bfa1, and the N-terminal region of Co Tem1 is required for this interaction. We also tested the interaction of *S. cerevisiae* Tem1p with Co Bub2 and Co Bfa1. Yeast clones carrying Co $Bfa1_{full}$ grew in the presence of *S. cerevisiae* Tem1p on selective medium, suggesting that Co Bfa1 can interact with *S. cerevisiae* Tem1p, which lacks the conserved N terminus region of *C. orbiculare* Tem1. For control experiments, we also detected the interaction between Bfa1p and Tem1p of *S. cerevisiae* but did not detect an interaction between Bub2p and Tem1p of *S. cerevisiae*, consistent with published results in *S. cerevisiae* (Kim et al., 2008). Taken together, these results suggest that Co Bub2 forms a two-component GAP complex with Co Bfa1, and both Co Bub2 and Co Bfa1 interact with the GTPase Co Tem1 in *C. orbiculare*. Both Co Bub2 and Co Tem1 contain the N-terminal region that is conserved only in filamentous fungi, and these N-terminal regions of Co Bub2 and Co Tem1 are required for the interaction with Co Bfa1 and Co Bub2/Co Bfa1, respectively, suggesting that these N-terminal regions of Co Bub2 and Co Tem1 might have specific roles in filamentous fungi.

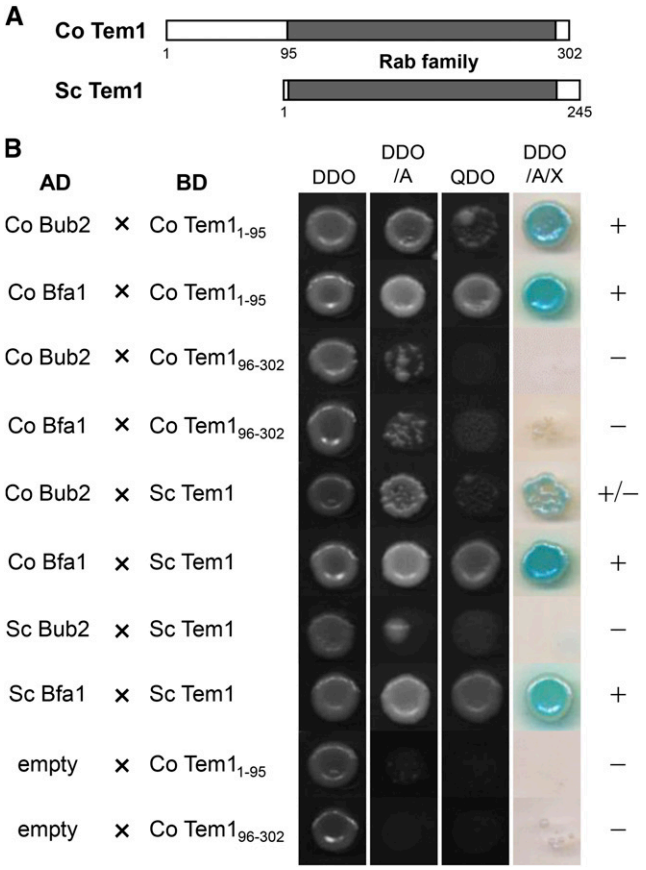

Figure 5. Co Tem1 Interacts with Co Bub2 and Co Bfa1 in Yeast Two-Hybrid Assays.

(A) Schematic representation of *C. orbiculare* Tem1 and *S. cerevisiae* Tem1p. The 95-amino acid sequence of the N-terminal end of Co Tem1 is specific to filamentous fungi and missing in yeast. Rab family domains of Co Tem1 and Tem1p are labeled in gray.

(B) Interaction of Co Tem1 with Co Bub2 or Co Bfa1 and interaction of *S. cerevisiae* Tem1p with Co Bub2 or Co Bfa1, as determined by a yeast two-hybrid experiment. Interaction was assessed from yeast growth on SD media lacking –Trp –Leu (DDO), –Trp –Leu + AbA (DDO/A), –Trp –Leu –Ade –His (QDO), and –Trp –Leu + AbA + X-α-Gal (DDO/A/X). The empty-AD vector was used as a negative control. +, Interaction; –, no interaction.

Co Tem1 Is a Downstream Target of Co Bub2/Co Bfa1 and Regulates G1/S Progression and Septum Formation

To investigate whether the two-component GAP Co Bub2/Co Bfa1 targets GTPase Co Tem1 to regulate G1/S progression in *C. orbiculare*, we generated a dominant-negative isoform of Co Tem1 analogous to the *S. pombe* homolog Spg1, a dominant-negative isoform, which has a Thr-to-Asn substitution at codon 24 (Schmidt et al., 1997). In *S. pombe*, the T24N mutant is predicted to titrate out the guanine nucleotide exchange factor and thus act as a dominant negative by inhibiting the signaling ability of the endogenous Spg1 (Schmidt et al., 1997). We then investigated whether Co *bub2Δ* and Co *bfa1Δ* expressing a dominant-negative form of Co Tem1 would restore the defective phenotype of G1/S arrest. A point mutation was generated in *C. orbiculare* Co Tem1 (Figure 6A), and the resulting allele was introduced by targeted allelic replacement into the *C. orbiculare* wild type and the Co *bub2Δ* and Co *bfa1Δ* mutants. The introduction of Co $Tem1^{T128N}$ restored the

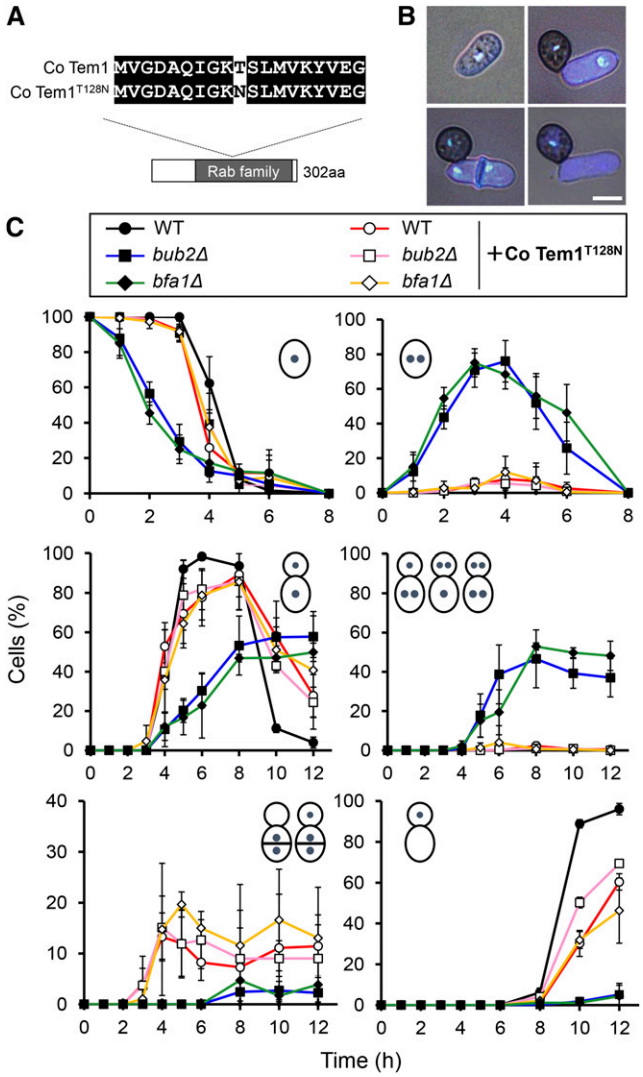

Figure 6. Introduction of Co Tem1^{T128N} Restored the Wild-Type Nuclear Behavior in Co *bub2Δ* and Co *bfa1Δ*.

(A) Schematic representation of the Co Tem1^{T128N} allele, which was introduced into wild-type *C. orbiculare* and Co *bub2Δ* and Co *bfa1Δ* mutants. **(B)** Representative images of nuclear distribution during appressorium morphogenesis in the Co Tem1^{T128N}-introduced strain. Pregermination conidia and appressorium-forming conidia were fixed and nuclei stained with DAPI and calcofluor white at 3 and 10 hpi, respectively. Bar = 5 μm. **(C)** Mean percentage (±SE; n = 3) of cells with various patterns of nuclear distribution for the wild type, Co *bub2Δ*, and Co *bfa1Δ*, with and without the introduced Co Tem1^{T128N} isoform. Lower left panel indicates conidia with two or three nuclei and an aberrant extra septum in the middle. For other scoring, see legend to Figure 1. At least 200 conidia were scored at each time point.

wild-type colony growth and restored conidia production, up to 40% over the very low conidia production in Co *bub2Δ* and Co *bfa1Δ* (Supplemental Table 1).

To investigate whether the nuclear behavior phenotype in Co *bub2Δ* and Co *bfa1Δ* is restored by introducing Co Tem1^{T128N}, we analyzed the nuclear behavior of Co Tem1^{T128N}-expressing transformants during appressorium differentiation. As expected, nuclear behavior was normal in most conidia from Co *bub2Δ* expressing Co Tem1^{T128N} and from Co *bfa1Δ* expressing Co Tem1^{T128N} (Figures 6B and 6C). While Co *bub2Δ* and Co *bfa1Δ* started nuclear division earlier and had more nuclei in the conidium and appressorium than in the wild type, most of the conidia from transformants expressing Co Tem1^{T128N} had normal nuclear division and subsequent distribution to the conidium and appressorium. In addition to the restoration of nuclear division, autophagy also proceeded normally in most conidia from Co Tem1^{T128N}-expressing transformants, while it was significantly delayed in Co *bub2Δ* and Co *bfa1Δ*. On the other hand, 20% of conidia from transformants expressing Co Tem1^{T128N}, including the wild type expressing Co Tem1^{T128N}, started nuclear division earlier and formed an aberrant extra septum at the middle of the germinating conidia. Since septa were rarely observed in germinating conidia of the wild type *C. orbiculare*, this result suggested that the Co *TEM1*^{T128N} allele might have a dominant effect on regulating nuclear division and septation.

To further characterize the function of Co Tem1, we generated Co *tem1* disruption mutants (Supplemental Figure 3). Although most Co *tem1Δ* conidia started nuclear division at 4 hpi without the extra septum that is typical of the wild type during appressorium differentiation, ~20% of Co *tem1Δ* started nuclear division earlier in pregermination conidia and formed an aberrant extra septum at the middle of the germinating conidia (Supplemental Figure 7). This phenotype of Co *tem1Δ* was consistent with that of transformants expressing Co Tem1^{T128N}. The *S. pombe* homolog Spg1, one of the SIN components, positively regulates septum formation (Schmidt et al., 1997). When the aseptate phenotype in *S. pombe spg1* mutants and the aberrant extra septum in transformants expressing Co Tem1^{T128N} and Co *tem1Δ* are considered together, Co *TEM1* seems to be a negative regulator of septum formation, in contrast with the *spg1* homolog in *S. pombe*. Therefore, these results indicate that Co Tem1 regulates two pathways, that is, G1/S progression under the control of Co Bub2/Co Bfa1 and negative regulation in septum formation.

In *S. cerevisiae* and *S. pombe*, Co Tem1 homologs localize at spindle pole bodies (SPBs), and this localization is important for its function (Sohrmann et al., 1998; Bardin et al., 2000; Valerio-Santiago et al., 2013). We then analyzed the localization of Co Tem1 and investigated whether it associates with cell cycle progression during appressorium development in *C. orbiculare*. We constructed strains in which the Co *TEM1* gene was C-terminally tagged with GFP under the control of its native promoter. In the pregerminated wild-type cells, one distinct Co Tem1-GFP signal was detected at the nuclear envelope (Figure 7A) in ~50% of the cells (Figure 7B). In germinated conidia at 2 hpi, double Co Tem1-GFP signals appeared, and these signals were detected in ~90% of the cells at 3 hpi. At 4 hpi, mitosis completed and double Co Tem1-GFP signals were symmetrically localized at both mother and daughter nuclei. To confirm that Co Tem1-GFP localizes to the SPBs, we observed Co Tem1-GFP in relation to α-Tubulin-mRFP signals. Microscopy observation demonstrated the colocalization of Co Tem1-GFP and α-Tubulin-mRFP during interphase and mitosis (Figure 7A). Especially during mitosis, Co Tem1-GFP signals were detected at both ends of mitotic spindle labeled by α-Tubulin-mRFP, suggesting that Co Tem1 localizes

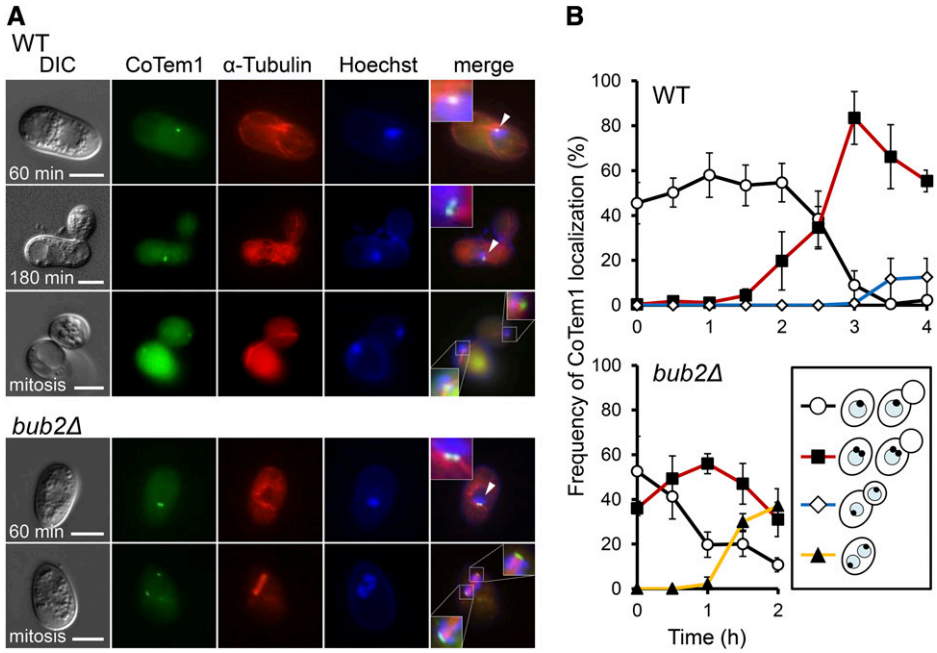

Figure 7. Co Tem1 Localization throughout the Cell Cycle during Appressorium Development.

(A) Representative images of the wild type and Co *bub2Δ* expressing Co Tem1-GFP and α-Tubulin-mRFP during appressorium development. Enlargement of Co Tem1 localization is shown in the boxed areas. Arrowheads indicate interphase nuclei. Nuclei was stained with Hoechst 33342. Bars = 5 μm.
(B) Mean percentage (±SE; $n = 3$) of cells expressing the *Co TEM1-GFP* gene fusion with four patterns of Co Tem1 localization. Scoring: single signal at one nucleus (black), double signals in one nucleus (red), and single signals at both nuclei after nuclear migration in appressorium developing conidia (blue) and in pregermination conidia (yellow). At least 100 conidia were scored at each time point.

SPBs throughout the cell cycle. Therefore, these results indicate that Co Tem1 localizes putative SPBs in a cell cycle-dependent manner. To elucidate whether the Co Tem1 localization was affected by Co Bub2/Co Bfa1, we visualized the *Co TEM1-GFP* gene fusion in the Co *bub2Δ* mutant. From the onset of conidial incubation, single or double Co Tem1-GFP signals were detected at the nucleus of most cells (Figure 7A), and the frequency of double Co Tem1-GFP signals increased by 1 hpi (Figure 7B). During mitosis in pregerminating conidia, Co Tem1 localized at both ends of spindle. These results suggest that the dynamics of the Co Tem1-GFP signal is affected by the absence of Co Bub2. Thus, Co Tem1 localizes at SPBs in a cell cycle-dependent manner and regulates proper G1/S progression in *C. orbiculare*.

Proper Cell Cycle Progression Is Required for Appressorium-Mediated Plant Invasion

To assess the requirement of Co *BUB2* and *Co BFA1* for fungal pathogenicity, we inoculated cucumber cotyledons with a conidial suspension of the mutants. In contrast to the distinct necrotic lesions induced by the wild type, Co *bub2Δ* and Co *bfa1Δ* induced either no lesions or occasional small lesions (Figure 8A). Microscopy observation revealed that more than 25% of the appressoria of the wild-type strain formed penetration hyphae, which invaded the host plant tissue by 3 d after inoculation (Figures 8B and 8C). By contrast, Co *bub2Δ* and Co *bfa1Δ* formed very few penetration hyphae. To confirm that the Co Bub2/Co Bfa1 cascade is involved in appressorial function, pathogenicity and infection-related morphogenesis on the host plant surface were examined in Co *bub2Δ* and Co *bfa1Δ* expressing Co Tem1^{T128N}. As expected, expression of Co Tem1^{T128N} restored both infection-related morphogenesis and pathogenicity on the cucumber cotyledons (Figures 8A and 8C). This result indicates that Co Bub2/Co Bfa1 is involved in appressorial function through the Co Tem1 signal cascade. From these results, we hypothesized that the attenuated pathogenicity of Co *bub2Δ* and Co *bfa1Δ* resulted from the defect in infection-related morphogenesis.

To investigate the relationship between cell cycle progression and appressorial penetration, we decided to focus on the septin and actin assemblies at the appressorium pore because they may provide rigidity to form the penetration peg. In *M. oryzae*, a septin assembly provides a scaffold for the toroidal F-actin network at the appressorium pore, a circular region from which the rigid penetration peg emerges (Dagdas et al., 2012). So we surmised that Co Bub2/Co Bfa1 affects the dynamics of the septins that might act as a scaffold for actin assembly at the appressorium pore, thereby causing the penetration defect in *C. orbiculare* mutants. To investigate this hypothesis, we visualized the septin cytoskeleton in Co *bfa1Δ* as a representative strain. A family of five septin genes has been identified in *M. oryzae*, and we expressed *M. oryzae SEP6-GFP* gene fusions in *C. orbiculare*. The Sep6-GFP signal showed dynamic localization during appressorium development (Supplemental Figure 8). We observed bright punctate structures in pregermination conidia, and after germination, the

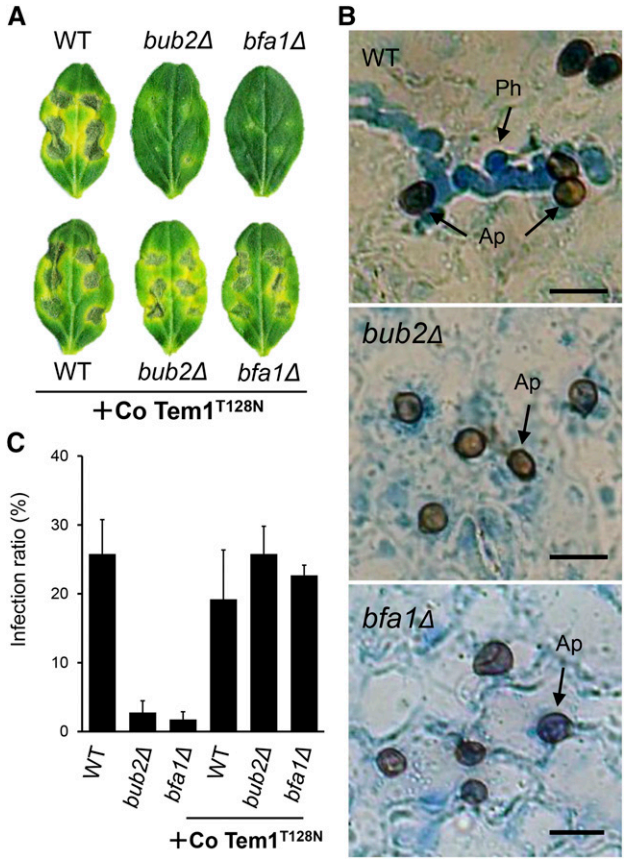

Figure 8. Defective Virulence of Co *bub2Δ* and Co *bfa1Δ* on Cucumber and Virulence Restored by Introduction of Co Tem1^{T128N}.

(A) Disease symptoms with dark, yellowish sunken necrosis on cucumber cotyledon infected with *C. orbiculare* wild type, Co *bub2Δ*, Co *bfa1Δ*, and the introduced Co Tem1^{T128N} isoform. Conidial suspensions were dropped onto a detached cucumber cotyledon and incubated at 24°C for 7 d.

(B) Micrographs showing penetration hyphae only in the wild type, not in Co *bub2Δ*, and Co *bfa1Δ*, on the lower surface of the cotyledon at 3 d after inoculation. Penetration hyphae were stained with lactophenol aniline blue. Ap, appressoria, Ph, penetration hyphae. Bars = 10 μm.

(C) Mean percentage (+SE; n = 3) of appressoria forming penetration hyphae. At least 200 appressoria were scored.

signal was observed at the tip of immature appressoria. In the mature appressorium, the Sep6-GFP signal was observed as an assembled spot at the neck of the appressorium. When we compared Sep6-GFP localization in Co *bfa1Δ* with that of the wild type, the frequency of localization of Sep6-GFP in Co *bfa1Δ* was greater, especially at the neck, the site of septation during cytokinesis. This result suggests that Co *bfa1Δ* is defective in completing cytokinesis in conidia and the processes for the development of the appressoria.

To assess the dynamics of the septins at the appressorium pore, we compared the localization of Sep6-GFP in Co *bfa1Δ* with that in the wild type. The wild type formed a distinct, narrow appressorium pore, where the Sep6-GFP signal was bright and punctate (Figures 9A and 9B). By contrast, Co *bfa1Δ* expressing Sep6-GFP formed a rather opaque and larger appressorium pore, where the Sep6-GFP signal was weaker than in the wild type. This result suggests that Co *bfa1Δ* has defects in assembling the septins at the appressorium pore.

To further investigate whether septin dynamics affect actin assembly at the appressorium pore, we visualized actin during appressorium development. As expected, the localization frequency of Lifeact-RFP at the appressorium pore was reduced, and the signal intensity was mostly fainter in Co *bub2Δ* and Co *bfa1Δ* than in the wild type (Figures 9A and 9C). These results indicate that the assembly of septin and actin at the appressorium pore was disturbed in Co *bub2Δ* and Co *bfa1Δ*.

Finally, we evaluated the possibility that the plant defense response is involved in the attenuated pathogenesis of Co *bub2Δ* and Co *bfa1Δ*. Unexpectedly, at sites of attempted penetration by Co *bub2Δ* and Co *bfa1Δ*, 80% of appressoria were accompanied by callose deposits, which were considerably larger than those formed by the wild type (Figures 9D and 9E). When inoculated leaves were stained with 3,3′-diaminobenzidine (DAB) to detect the accumulation of reactive oxygen species (ROS), 50% of plant cells attacked by Co *bub2Δ* or Co *bfa1Δ* appressoria showed positive DAB staining, as opposed to 0% of those attacked by the wild type (Supplemental Figure 9). To further evaluate the involvement of a plant defense reaction, we assayed infection after inoculation with Co *bub2Δ* or Co *bfa1Δ* on cucumber leaves that had been heat-shocked to impair resistance (Tanaka et al., 2007). The lesion formation by Co *bub2Δ* and Co *bfa1Δ* was partially restored on the leaves subjected to heat shock treatment (Supplemental Figure 9). Conclusively, these data suggest that Co Bub2/Co Bfa1 is required for pathogenesis via Co Tem1 and that the attenuated pathogenicity of Co *bub2Δ* and Co *bfa1Δ* resulted from a defect in septin- and actin-mediated penetration and in inducing a plant defense response.

DISCUSSION

The Novel Function of *BUB2* and *BFA1* in G1/S Progression in *C. orbiculare*

In *S. cerevisiae*, Bub2p constitutes a Rab GAP two-component complex with Bfa1p, and the Bub2p/Bfa1p complex regulates MEN as several cell cycle checkpoint components, such as SPOC, SAC, and DDC, in response to the misoriented spindle, unattached spindle to the kinetochore, and damaged DNA, respectively (Wang et al., 2000; Hu et al., 2001). By contrast, in *S. pombe* and *A. nidulans*, homologs of *BUB2* and *BFA1* act as negative regulators of the SIN, which is required for the onset of septum formation. SIN signaling activity is tightly regulated to ensure proper coordination of mitosis and cytokinesis (Furge et al., 1998; Li et al., 2000; Kim et al., 2006). In contrast to the results obtained so far for model yeast and fungi, we showed here that *C. orbiculare* homologs of *BUB2* and *BFA1*, Co *BUB2* and Co *BFA1*, play a major role in phase progression from G1 to S. This novel finding is supported by the following results. First, a mutation of Co *bub2* and Co *bfa1* initiated earlier nuclear division and caused binucleation in the pregermination conidia. Second, experiments using the LacO/LacI-GFP chromosome tagging system indicated that Co *bub2Δ* and Co *bfa1Δ* are defective in G1/S arrest. Thus, disruption of Co *BUB2* and Co *BFA1* did not

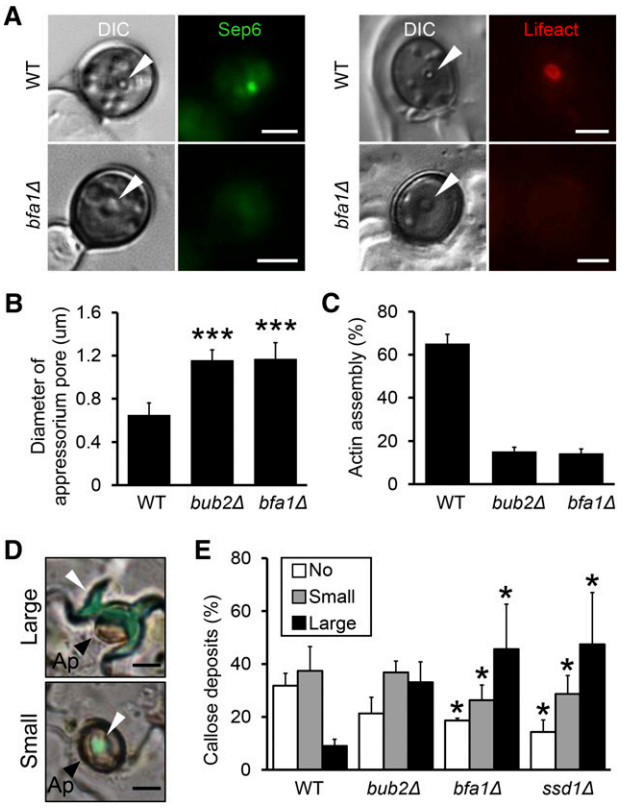

Figure 9. Co Bub2/Co Bfa1 Affects the Localization of Septin and Actin and the Defense Response of the Plant.

(A) Representative images showing septin and actin at the appressorium pore in the wild type and Co *bfa1Δ* during appressorium development. Strains harboring the *SEP6-GFP* gene were incubated on glass slides for 18 h, and strains harboring the *LIFEACT-RFP* gene were incubated on a cucumber cotyledon for 2 d. Arrowheads indicate appressorium pore. Bars = 2.5 μm.

(B) Diameter of the appressorium pore in the wild type, Co *bub2Δ*, and Co *bfa1Δ* with the *LIFEACT-RFP* gene (means + SE; $n = 4$). At least 50 appressoria were scored. Each strain was incubated on a cucumber cotyledon for 2 d. Asterisk represents significant differences between the wild type and each mutant (Student's *t* test; ***$P < 0.005$).

(C) Mean percentage (+SE; $n = 3$) of conidia that formed an actin assembly at the appressorium pore in the Co *bub2Δ* and Co *bfa1Δ* strain with the *LIFEACT-RFP* gene. At least 50 appressoria were scored. Each strain was incubated on a cucumber cotyledon for 2 d.

(D) Representative images of papillae with callose deposits at sites of attempted penetration by *C. orbiculare* appressoria. Large: callose formation larger than boundaries of the appressorium; small: callose deposits smaller than boundaries of the appressorium. Arrowheads indicate papillae. Ap, appressoria. Bars = 5 μm.

(E) Mean percentage (+SE; $n = 4$) of callose deposits at sites of attempted penetration by appressoria of the wild type, Co *bub2Δ*, Co *bfa1Δ*, and *Δcossd1* at 3 dpi. At least 400 appressoria were scored. Asterisk represents significant differences between the wild type and each mutant (Tukey's test; *$P < 0.05$).

significantly alter the phenotypes for mitotic exit or septum formation, while the primary functions of these homologs in *S. cerevisiae*, *S. pombe*, and *A. nidulans* are to inhibit the MEN or SIN signal cascade. From these phenotypic results, we wondered whether Co *BUB2* and Co *BFA1* are orthologs of *S. cerevisiae BUB2* and *BFA1*. A complementation test with *S. cerevisiae BUB2* and *BFA1* showed the restoration of proper G1/S progression in the Co *bub2Δ* Co *bfa1Δ* double mutant. Furthermore, the physical association of Co Bub2 with Co Bfa1 in a yeast two-hybrid assay confirmed that Co Bub2 forms a complex with Co Bfa1 similar to the Bub2p/Bfa1p GAP complex of *S. cerevisiae*. Therefore, we conclude that Co *BUB2* and Co *BFA1* are orthologs of *S. cerevisiae BUB2* and *BFA1* but have distinct roles in G1/S progression in *C. orbiculare*.

Co Tem1 GTPase Is a Downstream Target of Co Bub2/Co Bfa1 Rab GAP

In *S. cerevisiae* and *C. albicans*, the Bub2p/Bfa1p Rab GAP complex negatively regulates the direct downstream GTPase Tem1p, a component of MEN (Bardin and Amon, 2001; Milne et al., 2014). In *S. pombe* and *A. nidulans*, an analogous cascade SIN is conserved, and Cdc16/BUBA and Byr4/BYRA, homologs of Bub2p and Bfa1p, negatively regulate the downstream GTPase Tem1p homolog Spg1/ASGA (Furge et al., 1998; Li et al., 2000; Kim et al., 2006). The tightly regulated signal cascade of the two-component GAP and GTPase prompted us to question whether Co Bub2/Co Bfa1 regulates G1/S progression mediated by the Tem1 homolog Co Tem1 or another GTPase specific to *C. orbiculare*.

Our yeast two-hybrid experiments suggested that the N-terminal region of Co Tem1 is important for its association with the Co Bub2/Co Bfa1 GAP complex in *C. orbiculare*. However, in the case of the interaction of *C. orbiculare* Bub2/Bfa1 with *S. cerevisiae* Tem1p, Co Bfa1 associated with *S. cerevisiae* Tem1p, which does not contain the N-terminal region found in *C. orbiculare*. Thus, this difference in the Tem1 sequence and the association with the Bub2/Bfa1 GAP complex could be the reason for the difference in the cellular response between *C. orbiculare* and *S. cerevisiae*.

We introduced the T128N dominant-negative form of Co Tem1 into Co *bub2Δ* or Co *bfa1Δ* to test for complementation. Introduction of Co Tem1^{T128N} successfully complemented the defects of Co *bub2Δ* and Co *bfa1Δ* in the phase progression from G1 to S and autophagy, suggesting that Co Tem1 regulates G1/S progression through negative regulation by the Co Bub2/Co Bfa1 GAP complex. Thus, the two-component GAP Co Bub2/Co bfa1 seems to regulate G1/S progression through Co Tem1 in genetic and physical experiments.

Furthermore, we examined Co Tem1 localization during appressorium development. Co Tem1 localized to putative SPBs throughout cell cycle progression, and signal duplication of Co Tem1 increased from the onset of S phase, consistent with the duplication of SPBs reported in *S. cerevisiae* (Byers and Goetsch, 1975). In yeast, the homologs of Co Tem1 localize to SPBs and the localization affects MEN and SIN function (Sohrmann et al., 1998; Bardin et al., 2000). Therefore, Co Tem1 localization at SPBs was consistent with these reports, indicating that Co Tem1 regulates G1/S progression by localizing to SPBs.

A Role for Bub2/Bfa1 in Infection-Related Morphogenesis and Pathogenesis in *C. orbiculare*

The cell cycle is pivotal to cellular differentiation in multicellular eukaryotes, which must synchronize cell division to form specific

tissues and organs effectively (Kipreos, 2005; Théry and Bornens, 2006; Cools and De Veylder, 2009). Most plant pathogenic fungi develop appressoria to rupture plant cuticle and invade plant tissue. Cell cycle progression in plant pathogenic fungi is coordinately regulated to form proper infection structures. In *M. oryzae*, S phase is necessary to initiate appressorium differentiation, while M phase and autophagy in conidia are essential for the development of functional appressoria that form the penetration peg (Veneault-Fourrey et al., 2006; Saunders et al., 2010a). By contrast, in *U. maydis*, cell cycle arrest in G2 phase is required for the induction of appressorium formation, and the arrest is held until the infective dikaryotic hyphae penetrate host plants (Castanheira et al., 2014). Thus, *M. oryzae* and *U. maydis* have distinctive mechanisms of appressorium development that are coordinated with proper cell cycle progression. It was hypothesized that differences in appressorium development depend on the type of infection strategy adopted by appressoria (Castanheira and Perez-Martín, 2015). In one strategy, high turgor pressure enables cuticle penetration and, in the other, maintenance of heterokaryosis is required for successful infection. An analysis of microtubules dynamics in *C. orbiculare* during appressorium development indicates that precise nuclear distribution is required for proper appressorial development (Takano et al., 2001). However, a precise molecular genetic analysis of cell cycle regulation affecting infection-related morphogenesis and pathogenesis had not been reported for any *Colletotrichum* species.

For the *M. oryzae* appressorium to rupture the leaf cuticle, septin assemblies and an extensive toroidal F-actin network must be established at the appressorium pore (Dagdas et al., 2012). In Co *bub2Δ* and Co *bfa1Δ*, the frequency of septin and actin assembly was lower than in the wild type and some of the appressorium pores in the mutants were larger in diameter than were those of the wild type. This result indicates that the attenuated assembly of septin and actin in Co *bub2Δ* and Co *bfa1Δ* decrease cortical rigidly at the appressorium pore enough that the fungus cannot penetrate the host cuticle.

In addition to this functional attenuation of appressorium vigor, these mutants also unexpectedly induced an increased plant defense response, such as callose deposit and ROS accumulation, where the appressoria attempted to penetrate the plant cells. Heat-treated leaves of the host plant were unaffected by the defect of penetration ability of the Co *bub2Δ* and Co *bfa1Δ*, also suggesting that the mutant defect in forming disease lesions is associated with a host defense response. In *C. orbiculare*, the pexophagy-related mutant *coatg26* is defective not only in forming a penetration peg, but also in repressing the host defense response, thus leading to an inability to invade the host (Asakura et al., 2009). In *M. oryzae*, autophagy in the conidia was reported to have a pivotal role in the development of infection-related structures and for the avoidance of the plant immunity response (Talbot and Kershaw, 2009). Our analysis of Co *bub2Δ* and Co *bfa1Δ* showed that nuclei in the conidia were not degraded at the proper time, indicating a defect in autophagy.

Therefore, we propose that proper G1/S arrest by Co Bub2/Co Bfa1 during conidial germination is required to establish plant infection in *C. orbiculare*.

Global Regulation of Two-Component GAP and GTPase among Yeast and Filamentous and Dimorphic Fungal Species

Eukaryotes possess a wide variety of conserved proteins related to the cell cycle, but the function of the respective proteins may not always be identical among various species. Our study showed that

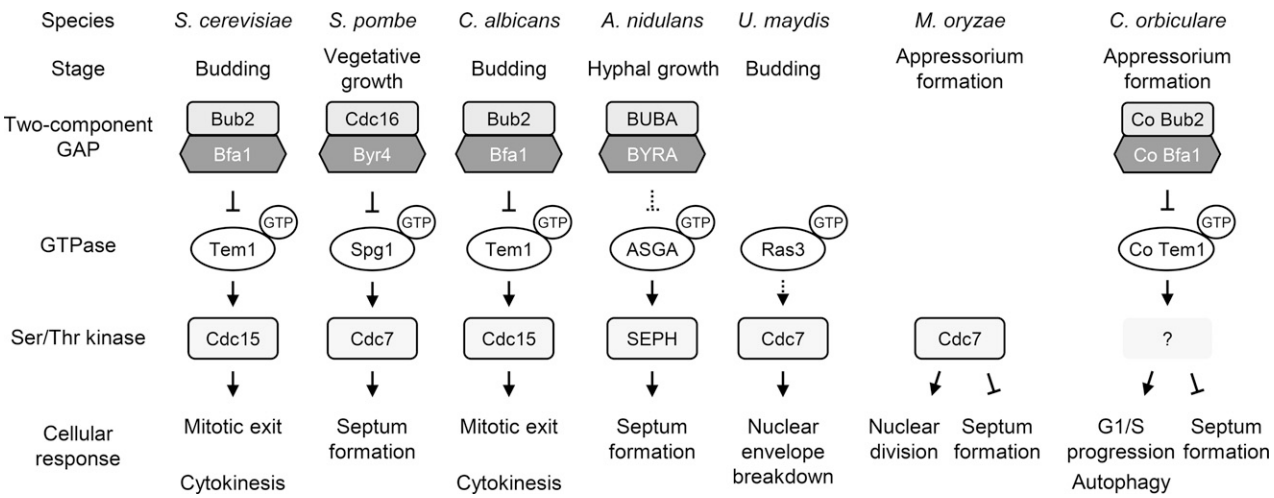

Figure 10. Model for Bub2/Bfa1 Functions and the Tem1 Pathways.

Schematic comparison of signaling networks of two-component GAP, GTPase, and Ser/Thr kinase and the subsequent cellular response in yeast and filamentous fungi. Whereas the signal cascade is widely conserved, the cellular response is diverse in *S. cerevisiae*, *S. pombe*, *C. albicans*, *A. nidulans*, *U. maydis*, *M. oryzae*, and *C. orbiculare*, regulating mitotic exit, septum formation, nuclear envelope breakdown, and G1/S progression. In *C. orbiculare*, Co Bub2/Co Bfa1 two-component GAP has a novel function that regulates G1/S progression, and autophagy via GTPase Co Tem1 and Co Tem1 negatively regulates septum formation.

the Bub2/Bfa1-Tem1 cascade is conserved between yeast and *C. orbiculare*; however, this signal cascade has different functions in yeast and in other filamentous fungi. Our results suggest that *C. orbiculare* has plant pathogen-specific roles for the two-component GAP and its GTPase that are involved in functional development in various yeast and fungal species (Figure 10). In *S. cerevisiae* and *C. albicans*, Bub2p/Bfa1p negatively regulates GTPase Tem1p, thereby triggering the MEN pathway, which controls mitotic exit and cytokinesis via Ser/Thr kinase Cdc15p (Bardin and Amon, 2001; Finley et al., 2008; Milne et al., 2014). A similar cascade, the SIN, has been reported in *S. pombe* and *A. nidulans*, and its primary role appears to be in regulating septation rather than mitotic exit (Bruno et al., 2001; Krapp and Simanis, 2008; Kim et al., 2009). By contrast, the Tem1 homolog in the plant-pathogenic basidiomycete fungus *U. maydis*, GTPase Ras3, is required for nuclear envelope breakdown during open mitosis via Cdc7 kinase (Straube et al., 2005). In ascomycete plant pathogens, the Ser/Thr kinase gene *SEP1*, a homolog of *S. cerevisiae CDC15*, was identified in *M. oryzae*, and its encoded protein both coordinates nuclear division and negatively regulates cytokinesis, functions that are required for successful appressorial penetration (Saunders et al., 2010b). In this study, we found that two-component GAP Bub2/Bfa1 of *C. orbiculare* regulates G1/S progression and autophagy via GTPase Tem1. Unlike yeast and fungal species, a mutation of Co *bub2* and Co *bfa1* did not impair mitotic exit or septation, but instead affected G1/S progression during appressorium development and led to penetration failure on the host plant. The observation that Co *Tem1*^{T128N} or Co *tem1Δ* mutants had an extra septum suggests that Co *TEM1* negatively regulates septum formation, consistent with the report from *M. oryzae sep1* mutants (Saunders et al., 2010b). However, this result is surprising because the homologs reported for yeast and other filamentous fungi positively regulate septum formation. Therefore, the signal cascade involving the two-component GAP and MEN/SIN components has been conserved, but the functions of the homologous genes in various species differ.

In conclusion, we consider that the Bub2/Bfa1 and Tem1 signaling cascade of *C. orbiculare* has been adapted for novel functional strategies to fulfill specific plant-pathogenic roles in different fungal species. Further investigation of Bub2/Bfa1 and Tem1 in other plant pathogens may provide insight into the diverse roles of these proteins in the cell cycle, which are likely to be necessary for virulence-associated processes in fungi.

METHODS

Strains and Growth Conditions

Strain 104-T (MAFF240422) of *Colletotrichum orbiculare* was used as the wild-type strain. All *C. orbiculare* strains were maintained at 24°C in darkness on 3.9% (w/v) potato dextrose agar (PDA) (Difco Laboratories) or SD medium (0.67% [w/v] yeast nitrogen base without amino acids, 2% [w/v] glucose, and 2% [w/v] agar). *Escherichia coli* DH5α-competent cells were used as a host for gene manipulation and maintained on Luria-Bertani medium at 37°C. *Agrobacterium tumefaciens* strain C58C1 was used as the T-DNA donor for fungal transformation and maintained on Luria-Bertani medium at 28°C.

Fungal Transformation

The AtMT protocol was applied with slight modifications of a previously described method (Tsuji et al., 2003). Hygromycin-resistant transformants were selected on PDA containing 100 μg/mL hygromycin B (Wako Chemicals) and 25 μg/mL meropenem hydrate (Sumitomo Dainippon Pharma). Bialaphos-resistant transformants were selected on SD medium containing 4 μg/mL bialaphos (Meiji Seika Kaisha) and 25 μg/mL meropenem hydrate. Sulfonylurea-resistant transformants were selected on SD medium containing 4 μg/mL chlorimuron ethyl (Maruwa Biochemical) and 25 μg/mL meropenem hydrate. For ectopic transformation of *C. orbiculare* with a fusion of Lac operator repeats and *M. oryzae SEP6-GFP* (Dagdas et al., 2012), polyethylene glycol-mediated protoplast transformation was performed as described previously (Kubo and Furusawa, 1991). All *C. orbiculare* strains generated in this study are listed in Supplemental Table 2.

Mutant Screening and Identification of *C. orbiculare* PDM1

Mutants of *C. orbiculare* PDM1 were screened using the AtMT protocol as described previously (Sakaguchi et al., 2010). The T-DNA inserted gene in the PDM1 mutant was identified using a thermal asymmetric interlaced-PCR protocol (Liu et al., 1995). Fungal genomic DNA flanking the T-DNA insert was analyzed as previously described (Tsuji et al., 2003). Amplified PCR products were sequenced with the Big-Dye Terminator Cycle Sequencing Ready Reaction Kit (Applied Biosystems) and an ABI PRISM 310 automated DNA sequencer (Applied Biosystems).

Gene Manipulations

For sequencing the entire region of the open reading frame of Co *BUB2*, Co *BFA1*, and Co *TEM1*, total RNA was extracted using the RNeasy Plant Mini Kit (Qiagen), and cDNA synthesis and subsequent PCR amplification were performed using ReverTra Ace (Toyobo). The oligo(dT)$_{12-20}$ primer was used for cDNA synthesis. Co *BUB2*, Co *BFA1*, and Co *TEM1* were amplified using the primers shown in Supplemental Table 3. The resulting cDNA was sequenced by Eurofins Genomics.

Genomic DNA of *C. orbiculare* was isolated from mycelia, and DNA gel blot analysis was done by standard methods. DNA probes were labeled with DIG-dUTP using the *Bca*BEST DIG labeling kit (Takara Bio). Hybridized DNA was detected using Anti-Digoxygenin-AP Fab fragments (Roche Diagnostics), and light emission generated by enzymatic dephosphorylation of CDP-Star Detection Reagent (GE Healthcare) and by alkaline phosphatase was detected using the FujiFilm LAS1000 plus gel documentation system.

Plasmid Construction

Plasmids were derived from the following binary vectors: pBIG4MRHrev, carrying the hygromycin resistance gene cassette; pBIG4MRBrev, carrying the bialaphos resistance gene cassette; pBIG4MRSrev and pCAMBIA-Sur-RfA, carrying the sulfonylurea resistance gene cassette; and pBIG4MRNrev, carrying the neomycin resistance gene cassette. For plasmid constructions, the In-Fusion HD cloning kit (Clontech) or GENEART Seamless cloning and assembly kit (Life Technologies) was used. All primers used in this study are listed in Supplemental Table 3.

To generate gene disruption mutants, plasmids in which cloned genes were replaced with the hygromycin resistance gene cassette were constructed. For generating the Co *bub2* disruption vector, a 1.0-kb fragment of the 5′ upstream region and a 1.0-kb fragment of the 3′ downstream region were amplified from *C. orbiculare* genomic DNA, and a 1.4-kb fragment of the hygromycin resistance gene was amplified from pBIG4MRHrev. These three fragments were inserted into a linearized pBIG4MRSrev. The same procedures were used to generate the Co *bfa1* disruption vector and the Co *tem1* disruption vector.

For chromosome tagging using lac operator/lac repressor system, two plasmids that contained the GFP-lac repressor fusions and lac operator repeats were constructed. To generate GFP-lac repressor fusion plasmids,

the 3.4-kp lacI-NLS-SV40 poly(A) fragment was amplified from the yeast vector pYN15 (Straight et al., 1996; Nabeshima et al., 1998), and the fragment was inserted at the C-terminal of GFP driven by *Aureobasidium pullulans TEF* promoter (Fujihara et al., 2010). To construct Lac operator repeat plasmids, the 2.8-kb sulfonylurea resistance gene cassette was digested with *Sal*I from pBIG4MRSrev and introduced into the *Sal*I-digested yeast vector pCT31, which carries the 10.2-kb 256 Lac operator repeats (Yamamoto and Hiraoka, 2003).

For complementation assays of the mutants, plasmids that contained the complete gene, native promoter, and terminator were constructed. To generate the Co *BUB2* complement vector, a Co *BUB2* fragment that contained 1.0 kb of the 5′ upstream region, the open reading frame, and 1.0 kp of 3′ downstream region was amplified from *C. orbiculare* genomic DNA. The fragment was inserted into a linearized pBIG4MRSrev. The same procedures were used to construct the Co *BFA1* complementation vector and the Co *TEM1* complementation vector.

For visualizing of *C. orbiculare* Histone H1 (Co His1) and Co Tem1, a plasmid that carries the gene encoding GFP regulated by the native promoter of Co *HIS1* or Co *TEM1* was constructed. For constructing the Co *HIS1-GFP* fusion gene vector, the Co *HIS1* complementation vector that carries the Co *HIS1* ORF with 1.0 kb of the 5′ upstream region and 1.0 kb of the 3′ downstream region was constructed. The GFP fragment was amplified from pBIglyGFP and inserted at the C-terminal end of Co His1 in the complementation vector. For constructing the *C. orbiculare* Co *TEM1-GFP* fusion gene vector, the GFP fragment was amplified from pBICoHIS1GFP and inserted at the C-terminal end of Co Tem1 in the Co *TEM1* complementation vector described above. For labeling microtubules, pBISCD1pmRFP1-α-TUB1S was used as previously described (Sakaguchi et al., 2008).

To complement the *C. orbiculare* mutants with *S. cerevisiae BUB2* and *BFA1*, the open reading frame of Co *BUB2* and Co *BFA1* was replaced with *S. cerevisiae BUB2* and *BFA1*, respectively. To construct the *S. cerevisiae BUB2*-replaced vector, the *BUB2* open reading frame was amplified from the *S. cerevisiae* DNA and replaced with the Co *BUB2* open reading frame in the Co *BUB2* complementation vector. The same plasmid construction strategy was used to generate the *S. cerevisiae BFA1*-replaced vector.

To generate a dominant-negative form of Co *TEM1*, a 516-bp fragment containing the upstream region of the Co *TEM1* open reading frame and a 522-bp fragment containing the downstream region of the Co *TEM1* open reading frame were amplified from *C. orbiculare* genomic DNA to generate a point mutation, which has an ACG-to-AAT substitution at codon 128. These two fragments were inserted into the pBIG4MRBrev binary vector. The sulfonylurea-selectable marker gene was amplified and inserted downstream of the 3′ untranslated region of Co *TEM1* in the Co *TEM1* point mutation plasmid.

Yeast Two-Hybrid Interaction Assays

The yeast two-hybrid screen was performed using the instructions of the Matchmaker Gold Yeast Two-Hybrid System (Clontech). Full-length cDNAs of putative interaction partners were generated from 3-d-old *C. orbiculare* mycelia. The genes encoding the proteins tested for interaction were cloned into the pGBKT7 or pGADT7 vectors (Clontech) to express fusion proteins with the yeast GAL4 binding (BD) and activation domain (AD), respectively. All BD or AD constructs were used to transform the Gold or Y187 yeast strain, respectively (Clontech). After mating, diploid yeast was plated on double dropout synthetic selective medium lacking Trp and Leu (DDO) for mating control and on stringent medium supplemented with 100 ng/mL aureobasidin A and 20 μg/mL X-α-Gal (DDO/A/X) and incubated at 28°C for 5 d. Protein interactions were assessed by growth of diploid yeast on DDO, DDO/A, DDO/A/X, and stringent quadruple dropout synthetic selective medium lacking Trp, Leu, Ade, and His (QDO) compared with corresponding controls (empty vectors).

Chemical Treatments

For staining nuclei of living cells, 2 μL of 100 μg/mL Hoechst 33342 (Dojindo Laboratories) was added to cells on samples on the glass slide and incubated for 10 min. For staining nuclei of fixed cells, samples were fixed with 3 to 4% (v/v) formaldehyde in 0.1 M phosphate buffer (pH 7.0) and 0.2% Triton X-100 at room temperature for 1 h. Fixed cells were then washed twice with 0.1 M phosphate buffer, and 1-μL of 1 μg/mL 4′,6-diamidino-2-phenylindole (DAPI; Sigma-Aldrich) was added directly to the cells on slides. For staining cell wall polysaccharides, 1-μL of 40 ng/mL Fluorescent Brightener 28 (Calcofluor white; MP Biomedicals) was added directly to the cells on slides. To examine penetration hyphae development in cucumber cotyledons, each sample was visualized using 0.1% lactophenol-aniline blue solution (Takano et al., 1997). For detecting callose deposits and ROS accumulation, each sample was stained with 0.01% (w/v) aniline blue in 0.15 M K_2HPO_4 and DAB (Yoshioka et al., 2003), respectively.

Pathogenicity Tests

C. orbiculare was tested for pathogenicity on detached cucumber cotyledons (*Cucumis sativus*) as described previously (Tsuji et al., 2003). Conidia of *C. orbiculare* were obtained from 7-d-old PDA cultures, and six drops of 10-μL of a conidial suspension (5×10^5 conidia/mL) were placed on the surface of cucumber cotyledons, and the tested strains were dropped onto five cucumber cotyledons. The cotyledons were incubated in a humid box at 24°C with a 16-h photoperiod for 7 d. For the heat shock treatment, detached cucumber cotyledons were dipped into distilled water at 50°C for 30 s and then inoculated with the test strains. For the control in all pathogenicity tests, distilled water was used instead of the conidial suspension.

Microscopy

For observation of appressorium formation, 20-μL of conidial suspension (10^5 conidia/mL 0.1% [w/v] yeast extract solution) was placed in the wells of multiwell glass slides (8-mm diameter; Matsunami Glass) and incubated in a humid environment at 24°C in the dark for 1 h. The yeast extract solution was then removed and replaced with distilled water. For observing penetration hyphae formation in vitro, a conidial suspension (10^5 conidia/mL distilled water) was placed on cellophane membranes (Wako Chemicals) and incubated at 24°C in the dark. For assessing penetration hyphae formation in planta, 10 μL of a conidial suspension (5×10^5 conidia/mL distilled water) was spotted onto the abaxial surface of cucumber cotyledons and incubated in a humid box at 24°C. After 3 d, we peeled off the lower epidermis of the cotyledons for observation on glass slides. For examining vegetative hyphae, the conidial suspension (10^5 conidia/mL 0.1% yeast extract solution) was placed on slides and incubated at 30°C.

Fluorescence was detected using a Zeiss Axio Imager M2 Upright microscope equipped with an AxioCam MRm digital camera and excitation/barrier filter set of 470 nm/509 nm for GFP and 595 nm/620 nm for RFP. Images were acquired with a 100× oil immersion lens (Plan Apochromat) using Axiovision 4.8 software. To observe the signal of GFP-lacI, 1.6× intermediate variable magnification was used. DAPI-stained and calcofluor white-stained samples were observed with a Nikon ECLIPSE E600 microscope equipped with a Keyence VB-7010 CCD color camera system. An excitation wavelength of 365/10 nm, dichroic mirror wavelength of 400 nm, and a barrier filter wavelength of 400 nm were used. Images were acquired with a 40× water immersion lens or a 100× oil immersion lens (Plan Fluor). To quantify the diameter of an appressorium pore, the images were analyzed using ImageJ (http://rsb.info.nih.gov/ij/).

Accession Numbers

Sequence data from this article can be found in the GenBank/EMBL databases under the following accession numbers: *C. orbiculare* Co Bub2

(ENH83696), Co Bfa1 (ENH87866), Co Tem1 (ENH82693), Co His1 (ENH76847); *Saccharomyces cerevisiae* Bub2 (NP_013771), Bfa1 (NP_012587), and Tem1 (NP_013647).

Supplemental Data

Supplemental Figure 1. Amino acid sequence alignment of Co Bub2 homologs.

Supplemental Figure 2. Amino acid sequence alignment of Co Bfa1 homologs.

Supplemental Figure 3. DNA gel blot analysis of targeted gene deletion mutants.

Supplemental Figure 4. Co *BUB2* is not involved in G1/S progression during vegetative hyphal growth in *C. orbiculare*.

Supplemental Figure 5. Amino acid sequence alignment of Co Tem1 homologs.

Supplemental Figure 6. Co Bub2 interacts with Co Bfa1 in yeast two-hybrid assays.

Supplemental Figure 7. Co *tem1Δ* is impaired in septum formation but not in nuclear behavior during appressorium development.

Supplemental Figure 8. Co Bub2/Co Bfa1 affects the localization of septin during appressorium development in *C. orbiculare*.

Supplemental Figure 9. A defense response in plants was induced by attempted penetration by appressoria of *C. orbiculare* mutants Co *bub2Δ* and Co *bfa1Δ*.

Supplemental Table 1. Growth rate and conidiation of mutants on PDA medium.

Supplemental Table 2. *Colletotrichum orbiculare* strains used in this study.

Supplemental Table 3. Primers used in this study.

Supplemental Table 4. *Saccharomyces cerevisiae* strains used in this study.

Supplemental Movie 1. Time-lapse imaging of nuclear division during appressorium development in wild-type *C. orbiculare*.

Supplemental Movie 2. Time-lapse imaging of nuclear division in pregermination conidia of *C. orbiculare bub2Δ*.

Supplemental Movie Legends.

ACKNOWLEDGMENTS

We thank N.J. Talbot and O.R. Miriam (University of Exeter, UK) for the Sep6-GFP vector of *M. oryzae*, A. Yamamoto (Shizuoka University, Japan) and A. Belmont (University of Illinois) for lac operator and GFP-lacI plasmid, Y. Nishizawa and M. Nishimura (National Institute of Agrobiological Sciences, Japan) for pCAMBIA-Bar-RfA, and G. Tsuji (Kyoto Prefectural University, Japan) for the Lifeact-RFP vector. We thank B.E. Hazen for carefully reading the article and giving valuable suggestions. This work was supported by Grants-in-Aid for Scientific Research from the Ministry of Education, Culture, Sports, Science, and Technology (Grants 24248009, 15H05780, and KH20140023) and by the Mitsubishi Foundation (No. 24110).

AUTHOR CONTRIBUTIONS

F.F. designed and performed the research, analyzed the data, and wrote the article. Y.K. designed the research, analyzed the data, and wrote the article.

Received February 26, 2015; revised June 30, 2015; accepted August 10, 2015; published August 28, 2015.

REFERENCES

Asakura, M., Ninomiya, S., Sugimoto, M., Oku, M., Yamashita, S., Okuno, T., Sakai, Y., and Takano, Y. (2009). Atg26-mediated pexophagy is required for host invasion by the plant pathogenic fungus *Colletotrichum orbiculare.* Plant Cell **21:** 1291–1304.

Bardin, A.J., and Amon, A. (2001). Men and sin: what's the difference? Nat. Rev. Mol. Cell Biol. **2:** 815–826.

Bardin, A.J., Visintin, R., and Amon, A. (2000). A mechanism for coupling exit from mitosis to partitioning of the nucleus. Cell **102:** 21–31.

Bruno, K.S., Morrell, J.L., Hamer, J.E., and Staiger, C.J. (2001). SEPH, a Cdc7p orthologue from *Aspergillus nidulans*, functions upstream of actin ring formation during cytokinesis. Mol. Microbiol. **42:** 3–12.

Byers, B., and Goetsch, L. (1975). Behavior of spindles and spindle plaques in the cell cycle and conjugation of *Saccharomyces cerevisiae*. J. Bacteriol. **124:** 511–523.

Castanheira, S., Mielnichuk, N., and Pérez-Martín, J. (2014). Programmed cell cycle arrest is required for infection of corn plants by the fungus *Ustilago maydis.* Development **141:** 4817–4826.

Castanheira, S., and Pérez-Martín, J. (2015). Appressorium formation in the corn smut fungus *Ustilago maydis* requires a G2 cell cycle arrest. Plant Signal. Behav. **10:** e1001227.

Cools, T., and De Veylder, L. (2009). DNA stress checkpoint control and plant development. Curr. Opin. Plant Biol. **12:** 23–28.

Dagdas, Y.F., Yoshino, K., Dagdas, G., Ryder, L.S., Bielska, E., Steinberg, G., and Talbot, N.J. (2012). Septin-mediated plant cell invasion by the rice blast fungus, *Magnaporthe oryzae*. Science **22:** 1590–1595.

Finley, K.R., Bouchonville, K.J., Quick, A., and Berman, J. (2008). Dynein-dependent nuclear dynamics affect morphogenesis in *Candida albicans* by means of the Bub2p spindle checkpoint. J. Cell Sci. **112:** 466–476.

Fujihara, N., Sakaguchi, A., Tanaka, S., Fujii, S., Tsuji, G., Shiraishi, T., O'Connell, R., and Kubo, Y. (2010). Peroxisome biogenesis factor *PEX13* is required for appressorium-mediated plant infection by the anthracnose fungus *Colletotrichum orbiculare*. Mol. Plant Microbe Interact. **23:** 436–445.

Furge, K.A., Wong, K., Armstrong, J., Balasubramanian, M., and Albright, C.F. (1998). Byr4 and Cdc16 form a two-component GTPase-activating protein for the Spg1 GTPase that controls septation in fission yeast. Curr. Biol. **8:** 947–954.

Gan, P., Ikeda, K., Irieda, H., Narusaka, M., O'Connell, R.J., Narusaka, Y., Takano, Y., Kubo, Y., and Shirasu, K. (2013). Comparative genomic and transcriptomic analyses reveal the hemibiotrophic stage shift of *Colletotrichum* fungi. New Phytol. **197:** 1236–1249.

Geymonat, M., Spanos, A., Smith, S.J., Wheatley, E., Rittinger, K., Johnston, L.H., and Sedgwick, S.G. (2002). Control of mitotic exit in budding yeast. In vitro regulation of Tem1 GTPase by Bub2 and Bfa1. J. Biol. Chem. **277:** 28439–28445.

Harata, K., and Kubo, Y. (2014). Ras GTPase activating protein Colra1 is involved in infection-related morphogenesis by regulating cAMP and MAPK signaling pathways through CoRas2 in *Colletotrichum orbiculare.* PLoS One **9:** e109045.

Harrison, J.C., and Haber, J.E. (2006). Surviving the breakup: the DNA damage checkpoint. Annu. Rev. Genet. **40:** 209–235.

Hu, F., and Elledge, S.J. (2002). Bub2 is a cell cycle regulated phospho-protein controlled by multiple checkpoints. Cell Cycle **1:** 351–355.

Hu, F., Wang, Y., Liu, D., Li, Y., Qin, J., and Elledge, S.J. (2001). Regulation of the Bub2/Bfa1 GAP complex by Cdc5 and cell cycle checkpoints. Cell **107:** 655–665.

Kim, J., Jang, S.S., and Song, K. (2008). Different levels of Bfa1/Bub2 GAP activity are required to prevent mitotic exit of budding yeast depending on the type of perturbations. Mol. Biol. Cell **19:** 4328–4340.

Kim, J.M., Lu, L., Shao, R., Chin, J., and Liu, B. (2006). Isolation of mutations that bypass the requirement of the septation initiation network for septum formation and conidiation in *Aspergillus nidulans.* Genetics **173:** 685–696.

Kim, J.M., Zeng, C.J., Nayak, T., Shao, R., Huang, A.C., Oakley, B.R., and Liu, B. (2009). Timely septation requires SNAD-dependent spindle pole body localization of the septation initiation network components in the filamentous fungus *Aspergillus nidulans.* Mol. Biol. Cell **20:** 2874–2884.

Kipreos, E.T. (2005). *C. elegans* cell cycles: invariance and stem cell divisions. Nat. Rev. Mol. Cell Biol. **6:** 766–776.

Krapp, A., and Simanis, V. (2008). An overview of the fission yeast septation initiation network (SIN). Biochem. Soc. Trans. **36:** 411–415.

Kubo, Y., and Furusawa, I. (1991). Melanin biosynthesis: Prerequisite for successful invasion of the plant host by appressoria of *Colletotrichum* and *Pyricularia*. In The Fungal Spore and Disease Initiation in Plants and Animals, G.T. Cole and H.C. Hoch, eds (New York: Plenum Publishing), pp. 205–217.

Kubo, Y., and Takano, Y. (2013). Dynamics of infection-related morphogenesis and pathogenesis in *Colletotrichum orbiculare.* J. Gen. Plant Pathol. **79:** 233–242.

Li, C., Furge, K.A., Cheng, Q.C., and Albright, C.F. (2000). Byr4 localizes to spindle-pole bodies in a cell cycle-regulated manner to control Cdc7 localization and septation in fission yeast. J. Biol. Chem. **275:** 14381–14387.

Liu, Y.G., Mitsukawa, N., Oosumi, T., and Whittier, R.F. (1995). Efficient isolation and mapping of *Arabidopsis thaliana* T-DNA insert junctions by thermal asymmetric interlaced PCR. Plant J. **8:** 457–463.

Milne, S.W., Cheetham, J., Lloyd, D., Shaw, S., Moore, K., Paszkiewicz, K.H., Aves, S.J., and Bates, S. (2014). Role of *Candida albicans* Tem1 in mitotic exit and cytokinesis. Fungal Genet. Biol. **69:** 84–95.

Musacchio, A., and Salmon, E.D. (2007). The spindle-assembly checkpoint in space and time. Nat. Rev. Mol. Cell Biol. **8:** 379–393.

Nabeshima, K., Nakagawa, T., Straight, A.F., Murray, A., Chikashige, Y., Yamashita, Y.M., Hiraoka, Y., and Yanagida, M. (1998). Dynamics of centromeres during metaphase-anaphase transition in fission yeast: Dis1 is implicated in force balance in metaphase bipolar spindle. Mol. Biol. Cell **9:** 3211–3225.

Robinett, C.C., Straight, A., Li, G., Willhelm, C., Sudlow, G., Murray, A., and Belmont, A.S. (1996). In vivo localization of DNA sequences and visualization of large-scale chromatin organization using lac operator/repressor recognition. J. Cell Biol. **135:** 1685–1700.

Sakaguchi, A., Miyaji, T., Tsuji, G., and Kubo, Y. (2008). Kelch repeat protein Clakel2p and calcium signaling control appressorium development in *Colletotrichum lagenarium.* Eukaryot. Cell **7:** 102–111.

Sakaguchi, A., Tsuji, G., and Kubo, Y. (2010). A yeast *STE11* homologue *CoMEKK1* is essential for pathogenesis-related morphogenesis in *Colletotrichum orbiculare.* Mol. Plant Microbe Interact. **23:** 1563–1572.

Saunders, D.G.O., Aves, S.J., and Talbot, N.J. (2010a). Cell cycle-mediated regulation of plant infection by the rice blast fungus. Plant Cell **22:** 497–507.

Saunders, D.G.O., Dagdas, Y.F., and Talbot, N.J. (2010b). Spatial uncoupling of mitosis and cytokinesis during appressorium-mediated plant infection by the rice blast fungus *Magnaporthe oryzae.* Plant Cell **22:** 2417–2428.

Schmidt, S., Sohrmann, M., Hofmann, K., Woollard, A., and Simanis, V. (1997). The Spg1p GTPase is an essential, dosage-dependent inducer of septum formation in *Schizosaccharomyces pombe.* Genes Dev. **11:** 1519–1534.

Sohrmann, M., Schmidt, S., Hagan, I., and Simanis, V. (1998). Asymmetric segregation on spindle poles of the *Schizosaccharomyces pombe* septum-inducing protein kinase Cdc7p. Genes Dev. **12:** 84–94.

Straight, A.F., Belmont, A.S., Robinett, C.C., and Murray, A.W. (1996). GFP tagging of budding yeast chromosomes reveals that protein-protein interactions can mediate sister chromatid cohesion. Curr. Biol. **6:** 1599–1608.

Straube, A., Weber, I., and Steinberg, G. (2005). A novel mechanism of nuclear envelope break-down in a fungus: nuclear migration strips off the envelope. EMBO J. **24:** 1674–1685.

Takano, Y., Kubo, Y., Kuroda, I., and Furusawa, I. (1997). Temporal transcriptional pattern of three melanin biosynthesis genes, *PKS1*, *SCD1*, and *THR1*, in appressorium-differentiating and non-differentiating conidia of *Colletotrichum lagenarium.* Appl. Environ. Microbiol. **63:** 351–354.

Takano, Y., Oshiro, E., and Okuno, T. (2001). Microtubule dynamics during infection-related morphogenesis of *Colletotrichum lagenarium.* Fungal Genet. Biol. **34:** 107–121.

Talbot, N.J., and Kershaw, M.J. (2009). The emerging role of autophagy in plant pathogen attack and host defence. Curr. Opin. Plant Biol. **12:** 444–450.

Tanaka, S., Yamada, K., Yabumoto, K., Fujii, S., Huser, A., Tsuji, G., Koga, H., Dohi, K., Mori, M., Shiraishi, T., O'Connell, R., and Kubo, Y. (2007). *Saccharomyces cerevisiae SSD1* orthologues are essential for host infection by the ascomycete plant pathogens *Colletotrichum lagenarium* and *Magnaporthe grisea.* Mol. Microbiol. **64:** 1332–1349.

Théry, M., and Bornens, M. (2006). Cell shape and cell division. Curr. Opin. Cell Biol. **18:** 648–657.

Tsuji, G., Fujii, S., Fujihara, N., Hirose, C., Tsuge, S., Shiraishi, T., and Kubo, Y. (2003). *Agrobacterium tumefaciens*-mediated transformation for random insertional mutagenesis in *Colletotrichum lagenarium.* J. Gen. Plant Pathol. **69:** 230–239.

Valerio-Santiago, M., de Los Santos-Velázquez, A.I., and Monje-Casas, F. (2013). Inhibition of the mitotic exit network in response to damaged telomeres. PLoS Genet. **9:** e1003859.

Veneault-Fourrey, C., Barooah, M., Egan, M., Wakley, G., and Talbot, N.J. (2006). Autophagic fungal cell death is necessary for infection by the rice blast fungus. Science **312:** 580–583.

Wang, Y., Hu, F., and Elledge, S.J. (2000). The Bfa1/Bub2 GAP complex comprises a universal checkpoint required to prevent mitotic exit. Curr. Biol. **10:** 1379–1382.

Yamamoto, A., and Hiraoka, Y. (2003). Monopolar spindle attachment of sister chromatids is ensured by two distinct mechanisms at the first meiotic division in fission yeast. EMBO J. **22:** 2284–2296.

Yeh, E., Skibbens, R.V., Cheng, J.W., Salmon, E.D., and Bloom, K. (1995). Spindle dynamics and cell cycle regulation of dynein in the budding yeast, *Saccharomyces cerevisiae.* J. Cell Biol. **130:** 687–700.

Yoshioka, H., Numata, N., Nakajima, K., Katou, S., Kawakita, K., Rowland, O., Jones, J.D., and Doke, N. (2003). *Nicotiana benthamiana* gp91^{phox} homologs *NbrbohA* and *NbrbohB* participate in H_2O_2 accumulation and resistance to *Phytophthora infestans.* Plant Cell **15:** 706–718.